



BNL-104207-2014-TECH

AGS.SN335;BNL-104207-2014-IR

SBE Beam Profile

M. Tanaka

June 1995

Collider Accelerator Department
Brookhaven National Laboratory

U.S. Department of Energy

USDOE Office of Science (SC)

Notice: This technical note has been authored by employees of Brookhaven Science Associates, LLC under Contract No.DE-AC02-76CH00016 with the U.S. Department of Energy. The publisher by accepting the technical note for publication acknowledges that the United States Government retains a non-exclusive, paid-up, irrevocable, world-wide license to publish or reproduce the published form of this technical note, or allow others to do so, for United States Government purposes.

DISCLAIMER

This report was prepared as an account of work sponsored by an agency of the United States Government. Neither the United States Government nor any agency thereof, nor any of their employees, nor any of their contractors, subcontractors, or their employees, makes any warranty, express or implied, or assumes any legal liability or responsibility for the accuracy, completeness, or any third party's use or the results of such use of any information, apparatus, product, or process disclosed, or represents that its use would not infringe privately owned rights. Reference herein to any specific commercial product, process, or service by trade name, trademark, manufacturer, or otherwise, does not necessarily constitute or imply its endorsement, recommendation, or favoring by the United States Government or any agency thereof or its contractors or subcontractors. The views and opinions of authors expressed herein do not necessarily state or reflect those of the United States Government or any agency thereof.

<p>AGS Complex Machine Studies (AGS Studies Report No. 335) SBE Beam Profile</p>
<p>Study Period: June 16, 1995</p>
<p>Participants: M. Tanaka and S.Y. Zhang</p>
<p>Reported by: S.Y. Zhang</p>

SBE BEAM PROFILE

1 Summary

During the June 1995 single bunch extraction (SBE) run, single bunches with the intensity of $1.7 TP$ (1.7×10^{12} protons) were extracted at about $24 GeV$, and some beam profiles such as the bunch length and the transverse emittances were measured. Using the information from the programs of the magnetic cycle, the RF gap voltage, and the γ_t jump, estimates of the momentum spread, and both longitudinal and transverse emittances were obtained. Also the dispersion effect on the normalized transverse emittance were obtained. These information will be useful in improving future high intensity proton FEB/SBE operations.

2 Bunch Length and Momentum Spread

The bunch length was measured using the mountain range displays, which is shown in Fig.1. The display is started at $50 ms$ from T_0 , with each step of $3 ms$, and is ended at $1250 ms$, where the bunch is extracted. Owing to the filamentation introduced by the VHF, we observe that the bunch is roughly in a Gaussian with exception around the transition. A Gaussian distribution implies smoothed bunch, which is important in calculating the momentum spread. In Fig.2 the bunch length is shown, together with the adiabatic phase damping calculated by,

$$\Delta\phi_\ell \propto \left(\frac{-\eta\omega_0^2}{\beta^2 EV \cos \phi_S} \right)^{1/4} \quad (1)$$

where

ϕ_ℓ is the half bunch length in *rad*,

η is the frequency slip factor,

ω_0 is the angular revolution frequency,

β is the ratio of the particle and light velocity,

E is the total energy,

V is the RF gap voltage per ring,

ϕ_s is the synchronous phase.

During the acceleration period from 480 *ms* to the transition, the bunch length roughly matches the phase damping. The effect of the VHF to the bunch length can be clearly observed during the injection porch and after the transition.

Consider the normalized longitudinal phase space

$$\left\{ \Delta\phi, \frac{|\eta|\omega_{RF}}{\omega_S} \frac{\Delta p}{p} \right\} \quad (2)$$

where

$\Delta\phi$ is the phase deviation,

ω_{RF} is the RF frequency,

Δp is the momentum deviation.

Assuming smoothed distribution in phase space, the normalized phase space (2) offers a *numerical equality* between the phase extent and the energy deviation, i.e. let $\Delta\phi$ and Δp be the maximum phase and momentum deviations of the bunch, respectively, we have,

$$\Delta\phi = \frac{|\eta|\omega_{RF}}{\omega_S} \frac{\Delta p}{p} \quad (3)$$

Therefore the momentum spread can be calculated from the bunch length,

$$\left(\frac{dp}{p}\right)_M = \pm \frac{\omega_S \phi_\ell}{|\eta|\omega_{RF}} \quad (4)$$

where $(dp/p)_M$ is the bunch momentum spread corresponding to the half bunch length ϕ_ℓ . The momentum spread is shown in Fig.3, where since the bunch length is not measured continuously, the small circles are also plotted to indicate the momentum spread calculated from the measured bunch lengths. We note that around the transition the particle distribution is distorted from Gaussian and the smooth distribution is not guaranteed, therefore, the momentum spread calculated using (4) carries some error.

3 Longitudinal Emittance

Consider the canonical energy deviation used in the longitudinal phase space,

$$W = \frac{\Delta E}{\omega_{RF}} \quad (5)$$

With this canonical co-ordinates of the longitudinal phase space, the bunch area and height are in a unit of *eVs*, and are ready to compare with the conventional bucket area and height. Using the relation

$$\frac{\Delta E}{E} = \beta^2 \frac{\Delta p}{p} \quad (6)$$

and the equation (3), substituting $\Delta\phi = \pi$ for the stationary bucket, we get the bucket half height,

$$W_{BK} = \frac{\pi\beta^2 E\omega_S}{|\eta|\omega_{RF}^2} \quad (7)$$

Note that W_{BK} is slightly different from the standard stationary bucket half height, which is $2\beta^2 E\omega_S/|\eta|\omega_{RF}^2\sqrt{\cos\phi_S}$. Using W_{BK} , the longitudinal emittance, i.e. the bunch area A_{BH} , and also the bunch half height in the longitudinal phase space, W_{BH} , can be written as,

$$A_{BH} = W_{BK}\phi_\ell^2 \quad (8)$$

and

$$W_{BH} = W_{BK}\frac{\phi_\ell}{\pi} \quad (9)$$

respectively. The equations (8) and (9) are the same as the ones in [1], but in simpler forms. In writing these equations, the correction factors are dropped, which introduce less than 5% errors in these applications. The longitudinal emittance is shown in Fig.4. The bunch half height, together with the moving bucket half height, is shown in Fig.5. The bunch area and height over the ones of the moving bucket are shown in Fig.6, where the length ratio of the bunch over bucket is also shown for comparison.

4 Transverse Emittance

The IPM beam profiles for both horizontal and transverse are shown in Fig.7. The Gaussian fit σ_M , i.e. the measured standard deviation, is shown in Fig.8. Normalized emittance including 95% particles is calculated using,

$$\epsilon_N = \frac{6\sigma_M^2}{\beta(s)}(\beta\gamma) \quad (10)$$

where

$\beta(s)$ is the Twiss parameter, at the IPM it is taken as 22 m for both horizontal and vertical,

γ is the Lorentz factor.

The normalized emittances for both horizontal and transverse are shown in Fig.9. The rising of the normalized emittance during the acceleration is noticed, where the contribution of the momentum spread related dispersion in the horizontal is considered relevant. Note that this dispersion effect is relatively significant for the higher energy, since the momentum spread does not change much in the entire cycle, and the beam size shown in Fig.8 at the higher energy is much smaller than the ones at lower energy.

To calculate the effect of the momentum spread on the total emittance, the dispersion effect of the individual particle momentum spread dp/p has to be considered. The contribution of the dispersion to the measured beam size is written as,

$$\sigma_M^2 = \sigma^2 + D_p^2 \langle (\frac{dp}{p})^2 \rangle \quad (11)$$

where $\langle (dp/p)^2 \rangle$ is the mean square value of the momentum spread, and D_p is the dispersion function at the IPM, which we take as 2.2 m. We assume that the distribution of dp/p in the bunch is also a Gaussian, with the standard deviation σ_p . Consider that the bunch length is measured at about 10% to 15% of the line density peak value, and the momentum spread shown in Fig.3 is calculated from this bunch length, we take,

$$(\frac{dp}{p})_M = 2\sigma_p \quad (12)$$

Since a zero mean value for dp/p can be assumed, we get the following equation,

$$\langle (\frac{dp}{p})^2 \rangle = \text{variance}(\frac{dp}{p}) \equiv \sigma_p^2 \quad (13)$$

Using equations (12) and (13), the dispersion excluded normalized emittance is,

$$\epsilon_{NDE} = \frac{6(\sigma_M^2 - D_p^2(\frac{1}{2}(dp/p)_M)^2)}{\beta(s)} (\beta\gamma) \quad (14)$$

where the measured momentum spread $(dp/p)_M$ is the one shown in Fig.3. The dispersion excluded emittance is shown in Fig.10, which is quite different from the normalized emittance ϵ_N at the higher energy, and is somewhat flat during the entire cycle, as expected. This emittance is roughly between 50 to 150 π mm - mr.

5 Discussion

The dispersion due to the momentum spread is supposed to affect only the horizontal emittance. In the measurement, the normalized vertical emittance also shows the rising during the acceleration. To compare the rising rate, the energy variation and both horizontal and vertical normalized emittances, which are scaled the same as the energy level at the injection porch, are shown in Fig.11. We note that the horizontal and vertical emittances have about the same rising rate. This is tentatively explained by the linear $x - y$ coupling, which is believed to exist in the AGS. Skew quadrupoles in the machine can turn horizontal motion into vertical and vice versa.

One important factor in figuring out the transverse emittance is the IPM space charge introduced distortion. In general, this effect is stronger when the beam transverse size is smaller. It is observed in Fig.8 that the beam size becomes smaller at the later half of the cycle, therefore this effect may contribute to the normalized emittance during that portion. Note that the IPM space charge effect intends to overestimate the beam size below the critical value, which at the intensity of this measurement corresponds to the standard

deviation between 2 *mm* to 3 *mm* [2]. From Fig.8 we observe that both horizontal and vertical beam standard deviations are above this size. Therefore it seems that the IPM distortion is not a dominant factor in this measurement. It is worth mentioning that at high energy the vertical beam size is less than two thirds of the horizontal one. If the IPM distortion is a dominant factor, then one would expect a difference between the vertical and horizontal normalized emittance rising rates during the acceleration, which is not observed in Fig.11. More measurement, however, is definitely needed to get a better understanding on the beam profile measured by IPM.

Another factor relevant to the emittance is the beam displacement from the closed orbit, x_D , which contributes to the measured emittance in the following way,

$$\sigma_M^2 = \sigma^2 + \frac{x_D^2}{2} \quad (15)$$

In this measurement, the displacement can only come from the RF frequency error, which is small, therefore this effect is not important.

6 Acknowledgment

We would like to thank K. Brown, D. Gassner, and J. Skelly for the set up of the mountain range display and the IPM program in the measurement.

References

- [1] S. Ohnuma, Fermilab Report TM-1381, 1986.
- [2] R. Thern, 1987 Particle Accelerator Conf. p.646, 1987.

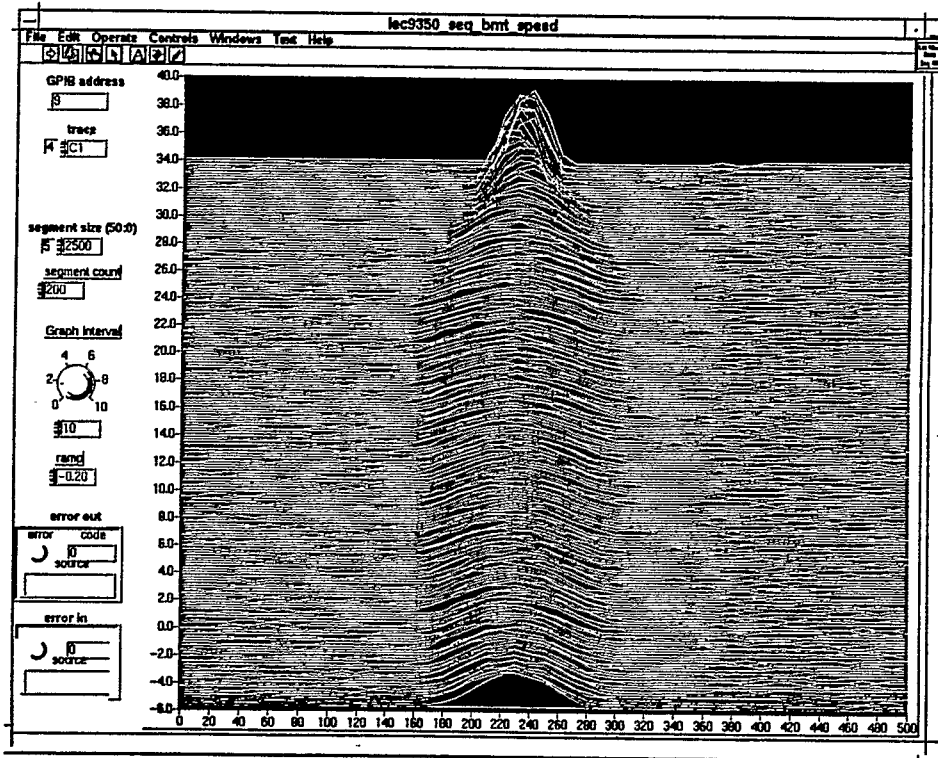
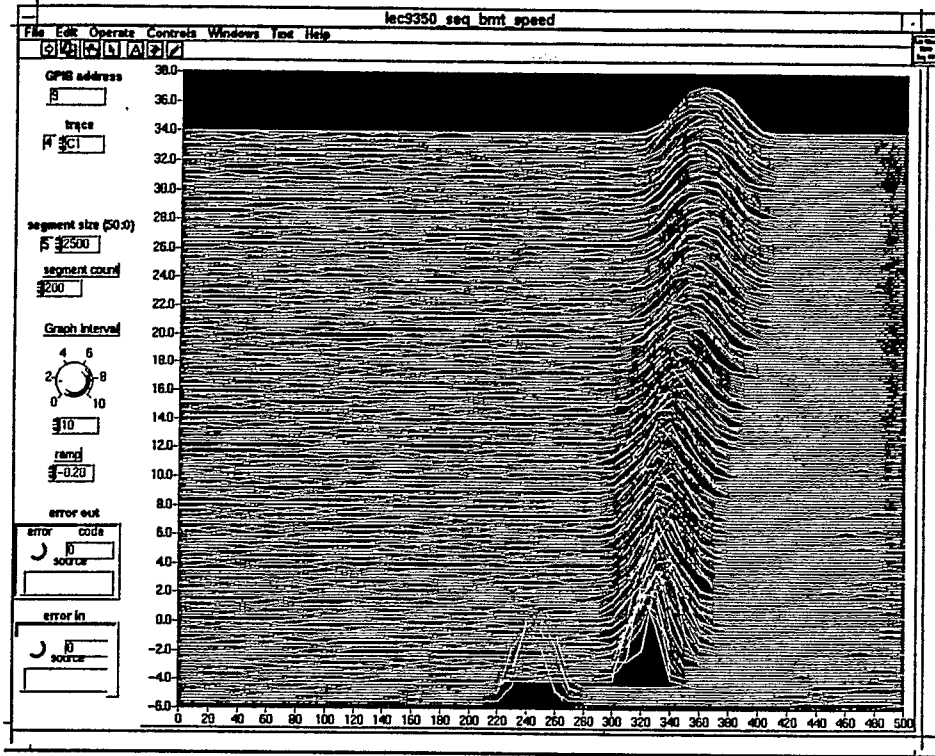


Fig.1. Mountain Range View

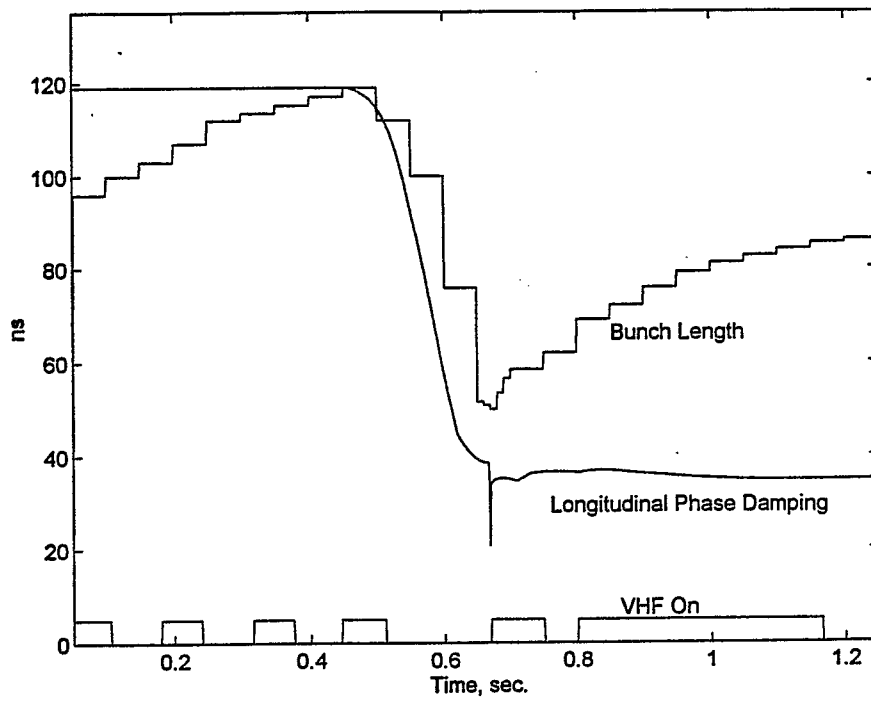


Fig.2. Bunch Length and Longitudinal Phase Damping

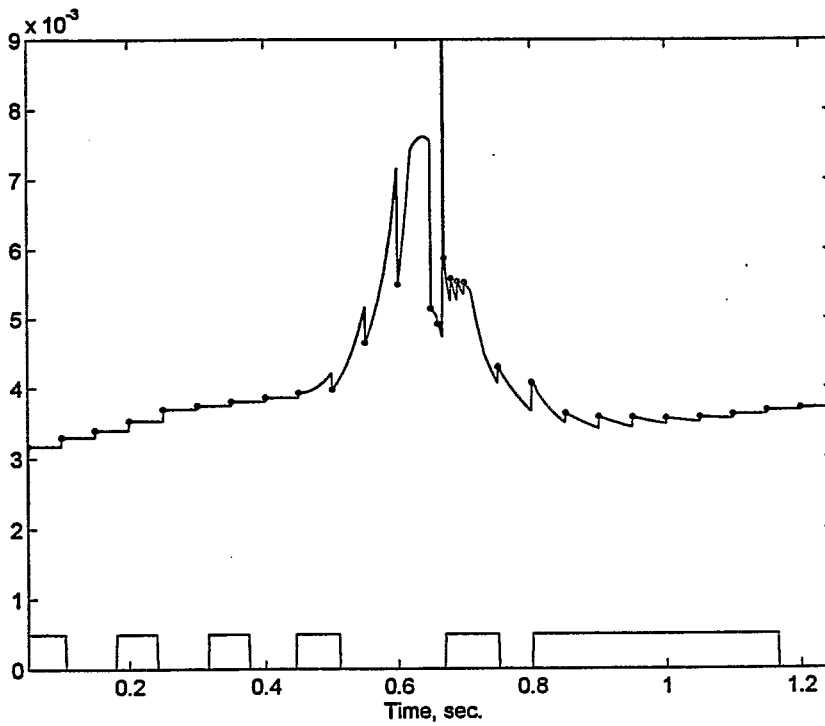


Fig.3. Momentum Spread

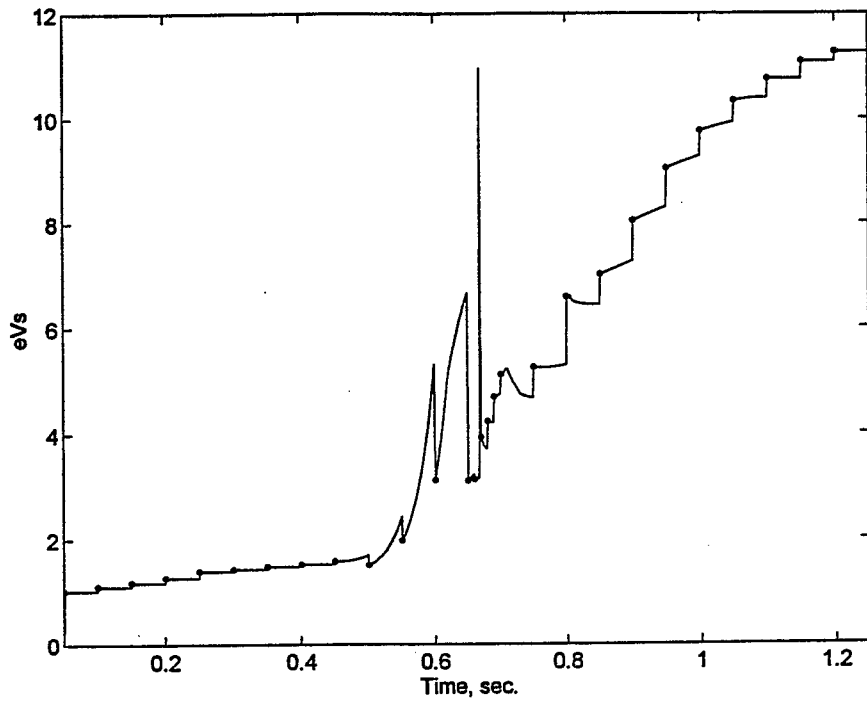


Fig.4. Longitudinal Emittance

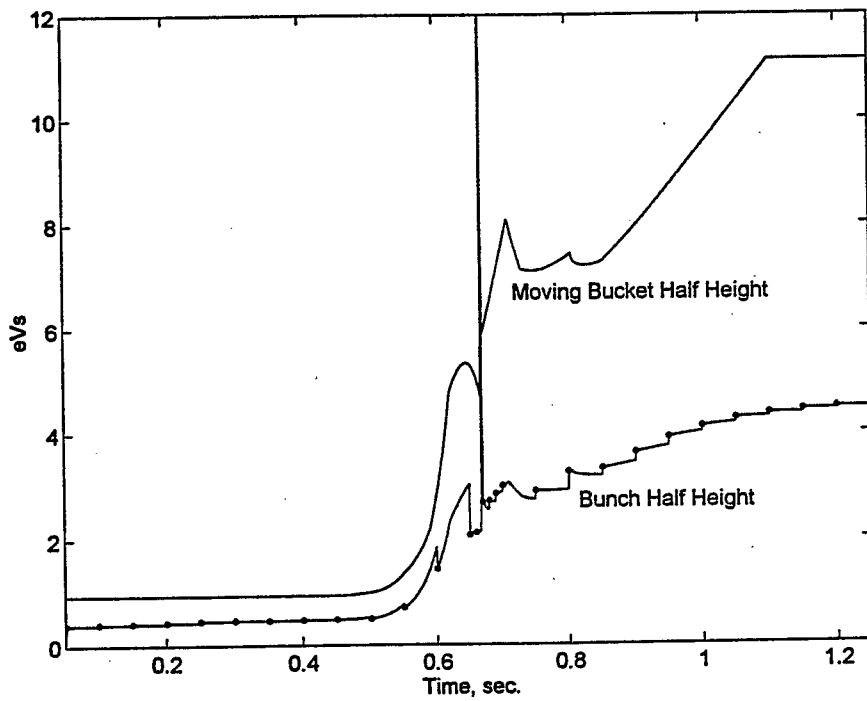


Fig.5. Bunch and Moving Bucket Half Heights

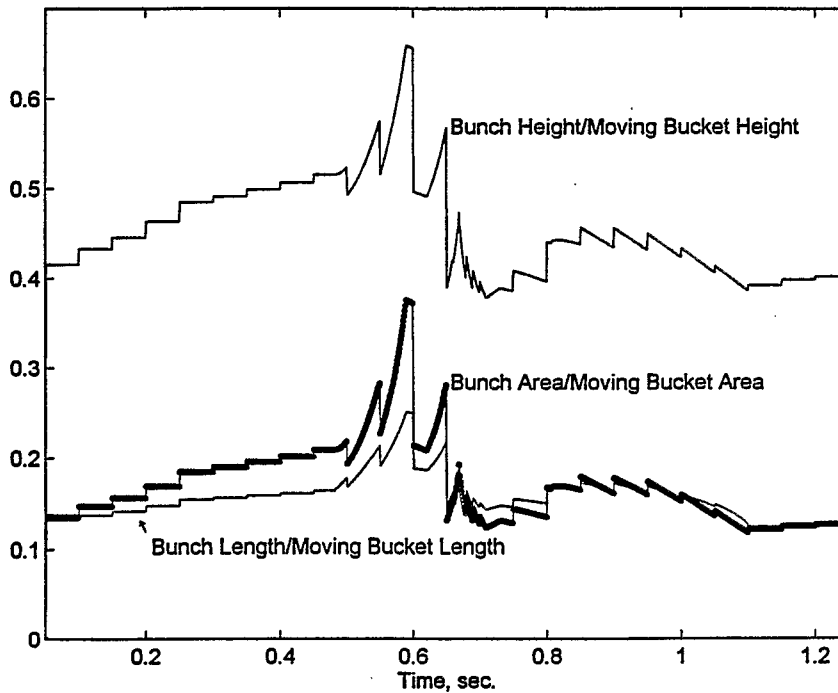


Fig.6. Comparison of Bunch and Moving Bucket Parameters

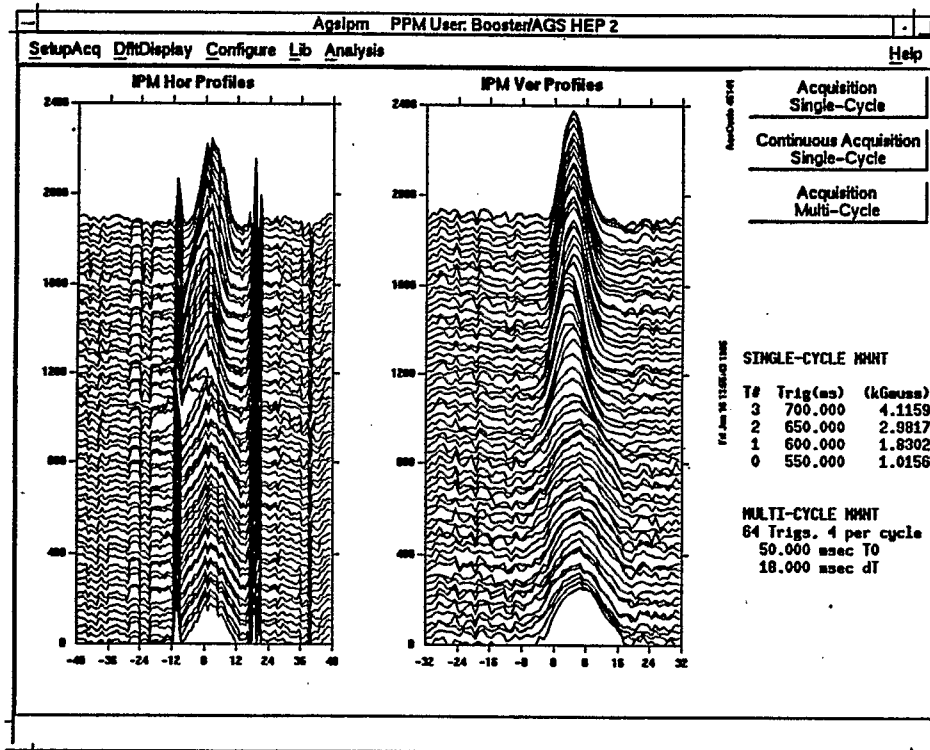


Fig.7. Transverse Beam Profile

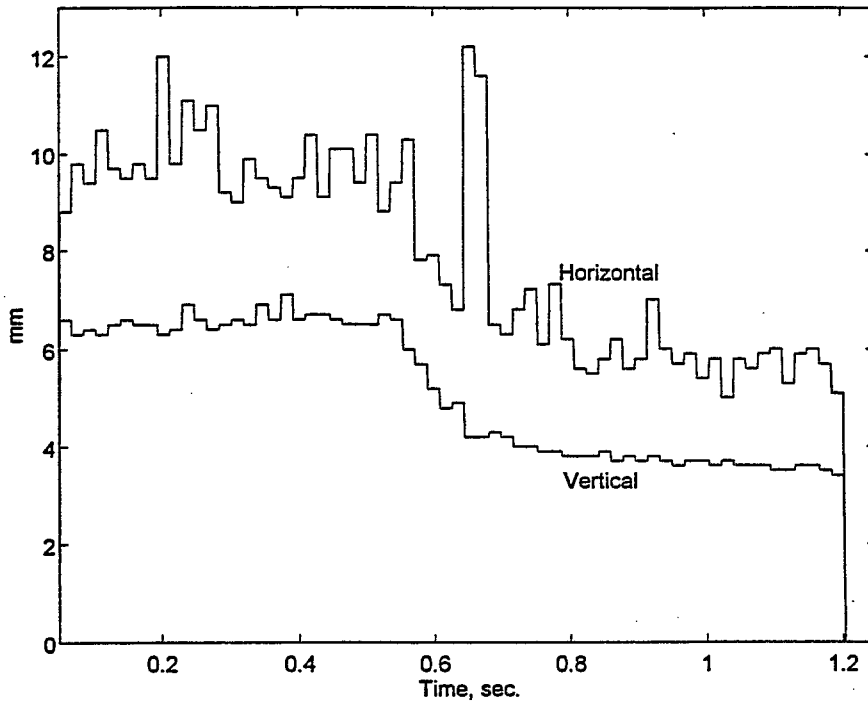


Fig.8. Horizontal and Vertical Sigma

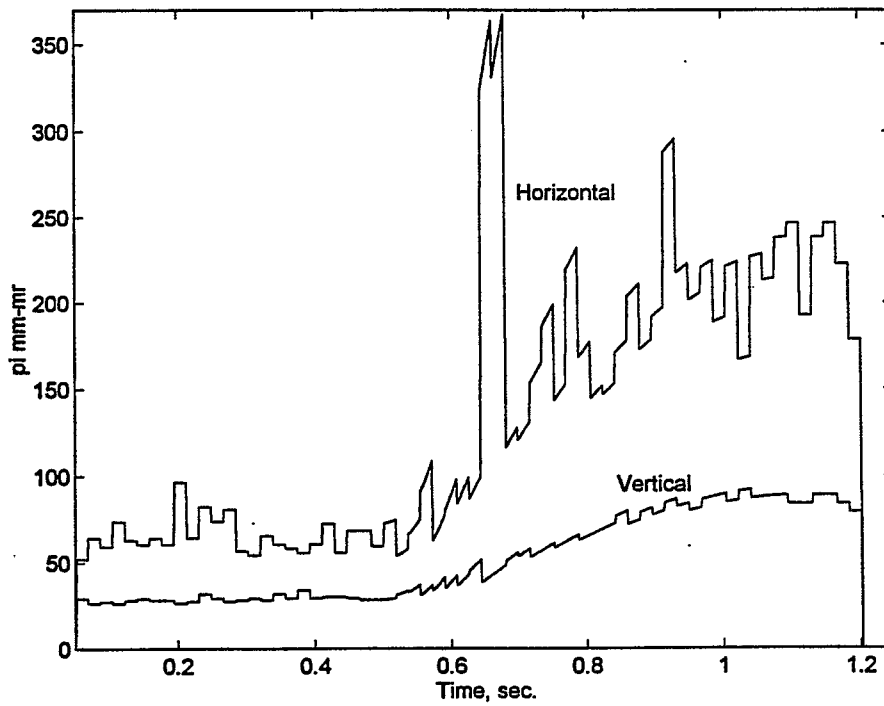


Fig.9. Normalized Transverse Emittance

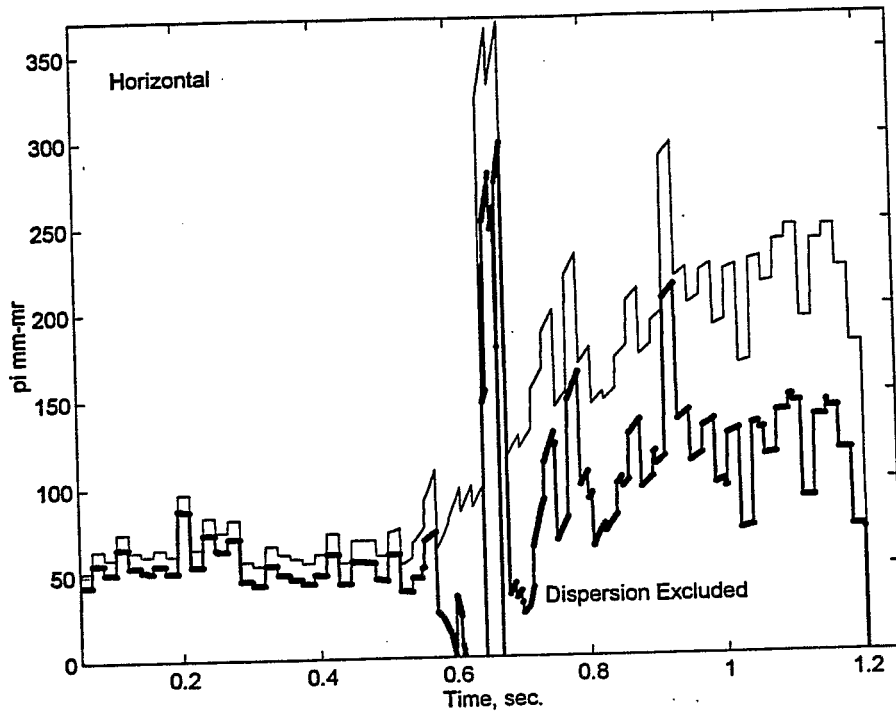


Fig.10. Dispersion Effect On Normalized Transverse Emittance

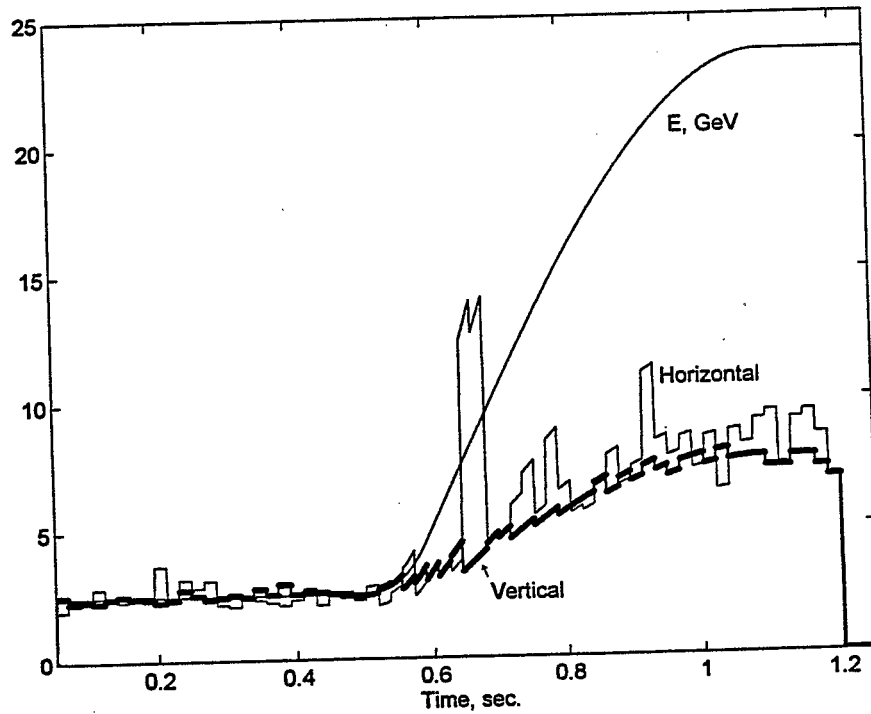


Fig.11. Normalized Emittance Variation Rates and Energy Increase